Does Epidemiology Matter? Policy Functions in Economic Epidemiological Models of Covid *

Aditya Goenka† Lin Liu‡ Haokun Pang §

September 9, 2024

Abstract

Economic epidemiology models have become a major application of dynamic general equilibrium theory to understand the interaction of infectious diseases and economic outcomes following the Covid pandemic. The papers have used differing assumptions of the epidemiology dynamics off-the-shelf from the epidemiology literature, where an unanswered question is what are the implications for optimal policies and the equilibrium outcomes of these assumptions. In a unified framework, we use both the Hamiltonian approach and a continuous time dynamic programming (HJB) approach to explore this issue. We numerically compute the policy and value functions under SIR (where recovery from an infection confers lasting immunity to subsequent infections) and SIRS (where it does not) dynamics. The value functions look qualitatively similar as does the policy function for consumption. However, the policy functions for the health expenditures differ. We present the phase portraits and the dynamics of the variables of interest. These differ greatly. We also conduct counterfactual analysis by assuming that the social planner misspecifies the epidemiology model by applying the health policy of SIR model to the pandemics with SIRS dynamics, and vice versa. We find the value loss of misspecifying the SIRS model is larger than that misspecifying the SIR model.

Keywords: Covid-19, optimal policies, SIRS, SIR, Long Covid, infectious diseases, NPI, growth model, value function, policy function, neural networks.

JEL Classification: *E13, E22, D15, D50, D63, I10, I15, I18, O41, C61.*

*We thank Raouf Boucekkine, Alex Citanna, Mich Tvede, and seminar participants in EWET Conference 2022, Naples; SAET Conference 2022, Paris; and ISI, Delhi for their helpful comments. The usual disclaimer applies

†Department of Economics, University of Birmingham, Email: a.goenka@bham.ac.uk

‡Management School, University of Liverpool, Email: lin.liu@liverpool.ac.uk

§Department of Economics, University of Birmingham, Email: h.pang.1@bham.ac.uk

I. Introduction

The Covid-19 pandemic led to a surge in economic epidemiological modelling. The economics literature not only looks at the interaction between the incidence of the disease with the economy but also generally studies optimal policies rather than compare simulations of different scenarios in the epidemiology literature (e.g. the influential papers by Flaxman et al. (2020) and Ferguson et al. (2020)). These models generally used Pontriagin's maximum principle to study the optimal control problem of how to control the morbidity and mortality from the pandemic while minimizing the economic loss. These models were generally parsimonious to avoid the curse of dimensionality and many did not model capital or used a partial equilibrium approach[1] where the economic variables such as consumption and interest rates are held fixed[2]. This paper uses a continuous time dynamic programming approach in a fully general equilibrium model (as in Goenka and Liu (2012); Goenka, Liu and Nguyen (2014); Goenka and Liu (2020); Goenka, Liu and Nguyen (2021, 2024)) so as to bring the modelling in parallel with standard macroeconomic modelling of economic fluctuations.

The use of dynamic programming enables the characterisation of the value and policy functions. The latter is especially important for Covid policymaking as it provides a clear guide for interventions as the state variables change. In the maximum principle approach, while the optimal trajectory can be calculated, it does not provide guidance if either some characteristics of the disease or the economic state variables were to change. However, the iteration-based dynamic programming technique (e.g. finite-differencing (Achdou et al., 2022)) usually suffer from the Curse of Dimensionality that the coding complexity and run time are exponential to number of state variables. We over come this curse by globally approximating the value function by deep learning neural networks (Fernández-Villaverde, Hurtado and Nuno, 2023; Fernandez-Villaverde et al., 2020). To increase the precision of the approximation, the steady state by the maximum principle method is used to guide the training of the network. We show the consistency between two approaches that the simulated path by neural network converges to the steady state solution by Hamiltonian.

The underlying economic model we use is the economic epidemiology model developed in Goenka, Liu and Nguyen (2021) where the state variables are the health states and capital. Covid-19 has two effects – mortality and morbidity. The earlier paper modelled both effects. By end of 2022, while morbidity remains significant, for most countries mortality from Covid-19 ceases to be of primary importance.

[1] E.g. Achdou et al. (2022), Alvarez, Argente and Lippi (2021).
[2] See i.e. Eichenbaum, Rebelo and Trabandt (2021).

The intervention we model are consumption reducing expenditures, which we label as health expenditure, that can decrease the likelihood of infections which includes social distancing.[3] While the earlier literature used SIR dynamics to model the disease dynamics, it has become clear that subsequent immunity to infections either from vaccines or prior infections is not long lasting so that SIRS dynamics are more appropriate.[4] In the paper, we analyse both SIR and SIRS dynamics as it also facilitates an understanding of how the details of epidemiology modelling will affect policies while taking into account the economic interactions.

A striking result is that the value functions and consumption policy functions for both the two epidemiology specifications look very similar, the policy function for health expenditures is very different in terms of their magnitudes. Moreover, when we look at the dynamics of the health components as well as consumption and health expenditures, they vary for the two different specifications. We further conduct counterfactual analysis by assuming that the social planner misspecifies the epidemiology model. Specifically, we assume that the health policy for SIR model is mistakenly applied when the disease actually follows the SIRS dynamics, and vice versa. As a result, we find the value loss from misspecifying the SIRS model is larger than that from misspecifying the SIR model, especially at the beginning of the pandemics.

As an extension we incorporate mortality from the disease. The total population would be affected by the path of excess infection-induced mortality. Thus, the discount rate is endogenous as a function of the cumulative excess mortality (Goenka, Liu and Nguyen, 2021, 2024). We do not avoid the endogenous discounting problem as Alvarez, Argente and Lippi (2021) who hold the population size constant and model the deceased in a new state where they do not consume or produce. Instead, as in (Goenka, Liu and Nguyen, 2021, 2024), we introduce an extra state variable for modelling the changing discount rate into value function.[5] The performance of our approximation is not much affected by the inclusion of the additional state variable as the deep learning technique enables us to handle high-dimensional dynamic programming problem.

From the control theoretic point of view, the sufficiency conditions of Arrow and Mangasarian fail in economic epidemiology models. For our model, the results in Goenka, Liu and Nguyen (2021) and Goenka, Liu and Nguyen (2024) cover the SIR and SIRS cases respectively. The dynamic programming approach side-steps this

[3] Goenka, Liu and Nguyen (2024) model optimal lockdowns but in this paper we do not model it as in the policy space the use of lockdowns looks unlikely going forward.

[4] See e.g. Cele et al. (2021); Hansen et al. (2021); Sabino et al. (2021); Cagigi et al. (2021) The SARS-Cov-2 virus is not a stable virus. The mutation is quick and hard to track. This further reduces the effectiveness of immunity that data shows the most reinfection happens among different variants of virus (ONS, 2023).

[5] This follows Uzawa (2017).

problem (see Calvia et al. (2024)) as concavity of the objective is retained but we do not need any such assumption on the evolution of the state variables.[6]

For modelling purposes we use continuous time rather than discrete time. From a practical level, it should not matter which assumption is used as it is just a matter of calibrating the model to the right frequency. However, the HJB approximation in the continuous time approach has better performance in both accuracy and efficiency Achdou et al. (2022). Furthermore, from a theoretical point of view, the disease dynamics in discrete time are unimodal so that if the contact rate is high enough, there can be cycles and chaos Goenka and Liu (2012). The pure epidemiology continuous time specification on the other hand does not admit endogenous fluctuations.[7] As estimates of the contact rate have varied dramatically over the pandemic[8], it would seem reasonable to use a continuous time specification as the time frequency should not become an independent source of complexity.

The plan of the paper is as follows. section II. outlines the economic epidemiology model. section III. numerically solves for the both the SIR and SIRS models the steady states, the value and policy functions, and the stable manifolds of the dynamical system. The difference between the dynamics of the two models is shown. section IV. applies the model to study the effect from vaccination. We also introduce Covid-induced mortality in this section.

II. The Economic Epidemiology Model

A. Model Setup

The model is based on the growth model with in Goenka and Liu (2012, 2020) and Goenka, Liu and Nguyen (2014, 2021, 2024). In this paper we use an underlying neoclassical growth model with epidemiological dynamics. We use model agents as large representative households to avoid keeping track of the history of health status.

Households. We assume the economy is populated by a continuum of non-atomic identical households who are the representative decision-making agents. The size of the population is $\mathcal{N}$. The total population grows over time at the rate of $b - d \geq 0$, where b is the birth rate and d is the natural death rate. Within each household, an individual is either healthy or infected or recovered from the diseases. We will introduce the epidemiology compartment in detail later.

We model the infectious disease as causing morbidity — reducing productivity of

[6]The sufficiency results cited above also rely on concavity of the objective function and sufficiency can be shown directly.

[7]See i.e. the discussion in Boucekkine et al. (2024).

[8]The variant BF.7 that is dominant in China in December 2022 has a reproduction rate 10.8-18.6. In 2020 it was estimated to be an average of 2.2 in Western Europe (Linka, Peirlinck and Kuhl, 2020).

the infected. We make the simplifying assumption that when an infected individual is incapacitated by the disease that the productivity falls to zero.[9] We further assume the labour is supplied inelastically.[10] The infectious disease externality, where individuals ignore the effect of their own actions on the dynamics of the disease, can have significant effects. In this paper we are interested in what a policymaker should do based on the state of the pandemic and thus, focus on the optimal policy.[11]

The objective for the representative household is to maximize the discounted utility

$$\int_0^\infty e^{-[\rho-(b-d)]t}u(c_t)dt, \tag{1}$$

where ρ is the discount factor with $\rho - b + d > 0$; c_t is the consumption. The size of household is assumed to be one. The growth rate of total population is $b - d$[12].

Assumption 1. *The utility function* $u : \mathbb{R}_+ \to \mathbb{R}$ *is* $\mathcal{C}^2$ *with* $u' > 0, u'' < 0$. *The discount rate* $\rho > b - d$.

Epidemiology and labour supply. The epidemiology model we use are the SIRS and SIR models. We assume that diseases follow the SIRS dynamics. The SIR dynamics will be a special case for SIRS with different parameterization. An individual can be in one of three health states: $\mathcal{S}$ – healthy and susceptible to the disease; $\mathcal{I}$ – infected and capable of transmitting infections, that is, infectious; $\mathcal{R}$ – recovered from the disease and having immunity from the disease. If there are vaccinations, then an individual has immunity to the disease without going through an infection. In this paper, we do not model vaccinations. However, as we will mention later, if we change initial conditions of the state variables in the model by increasing the fraction of $\mathcal{R}$ then one could interpret this as individuals having immunity from the disease either conferred from recovery from infections or from vaccinations.

In the epidemiology model, susceptible group get infected by contacting the infectious disease. The contact rate, which is key to determine the prevalence of infectious disease, is Poisson. We assume it is affected by health expenditure, that is, each household can control infection by investing in health expenditure $h = H/\mathcal{N}$.

[9] How much productivity is affected varies across diseases and see Goenka, Liu and Nguyen (2021) for a discussion of this. If we assume partial decrease in productivity the qualitative results are not affected.

[10] Goenka and Liu (2012) endogenized the labour-leisure choice with SIS disease dynamics and showed that the dynamics are invariant under standard assumptions.

[11] Goenka and Liu (2020) have a comprehensive discussion of the effects of the disease externality in a similar model but with SIS dynamics.

[12] In section IV., we introduce mortality. The population growth rate and the discount rate would be endogenous as functions of state variable.

Figure 1. Flow of Epidemiological Compartments

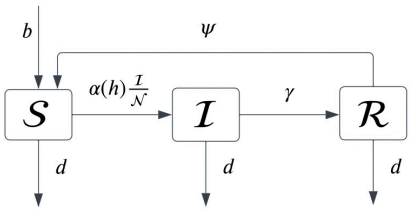

This can be thought of preventive measures taken to prevent the transmission of the disease. This is the specification used in Goenka and Liu (2012); Goenka, Liu and Nguyen (2014). The second paper also modeled expenditures that increase recovery rates from the disease but we abstract from this in this paper as there are no known therapies for recovery from Covid-19.[13] Eichenbaum, Rebelo and Trabandt (2021) interpret this loss of output, h, in our context, as the cost of a lockdown which also reduces the transmission rate α and thus, is also consistent with interpreting it as the cost of a lockdown which reduces transmission of the disease by forgoing output.[14]

Assumption 2. *The contact rate is a function of health expenditure h, i.e. $\alpha(h)$. We assume $\alpha' < 0; \alpha'' > 0$ and $\lim_{h\to 0} \alpha(h) = \bar{\alpha}$.*

For the recovery process, we assume the infected group recovers at an exogenous rate of γ. We analyse both SIRS and SIR model, where the key difference lies in the immunity for the recovered group. For the SIRS model, the recovered group would lose their immunity at some rate. We denote ψ as the rate of re-entering the susceptible group. In the SIR model, the immunity is life-long, implying $\psi = 0$. With the assumptions above, the flow of population in each compartment can be shown in Figure 1.

By normalizing the population in each compartment that

$$s = \frac{\mathcal{S}}{\mathcal{N}}; \quad i = \frac{\mathcal{I}}{\mathcal{N}}; \quad r = \frac{\mathcal{R}}{\mathcal{N}}. \tag{2}$$

we can have set of differential equations to represent the motion of the compartments as follow

[13] Antivirals and anti-inflammatory drugs are now known to reduce mortality but these are inexpensive and widely available prior to the outbreak. While ventilators are used in severe cases, there is an emerging view that their use can complicate recovery and in fact cause ventilator induced lung injury (Marini and Gattinoni, 2020).

[14] In Goenka, Liu and Nguyen (2024), we have a different way of modeling a lockdown or quarantine where a fraction of the non-infective population has to work from home with a reduced productivity.

$$\begin{aligned}\dot{s} &= b - bs - \alpha(h)si + \psi r,\\ \dot{i} &= \alpha(h)si - \gamma i - bi,\\ \dot{r} &= \gamma i - \psi r - br.\end{aligned} \tag{3}$$

Production. The production side of the model is a standard neoclassical growth model where households can invest in capital which is productive next period and depreciates at rate δ[15]. Households own representative firms that use capital and labour as inputs.

Assumption 3. *The production function $f(k,l)$, $f:\mathbb{R}^2_+ \to \mathbb{R}_+$ is $\mathcal{C}^2$ with*

1. $f_k > 0, f_l > 0$,
2. *f is concave and homogeneous of degree 1,*
3. $f(0,\cdot) = f(\cdot,0) = 0$,
4. $\lim_{k\to 0} f_k(k,\cdot) = \lim_{l\to 0} f_l(\cdot,l) = \infty$, $\lim_{k\to\infty} f_k(k,\cdot) = 0$,
5. *The physical capital depreciates at the rate $\delta \in [0,1]$.*

The law of evolution of capital stock is $\dot{K} = f(K, \mathcal{N} - \mathcal{I}) - C - H - \delta K$. We define for each household, physical capital per capita $k = K/\mathcal{N}$ and consumption per capita $c = C/\mathcal{N}$. The law of motion for physical capital per capita can be rewritten as:

$$\dot{k} = f(k, 1-i) - c - h - \delta k - (b-d)k. \tag{4}$$

B. Optimization Problem for Social Planner

The social planner maximizes the discounted utility Equation 1 subjected to the motion of capital Equation 4 and the motions of epidemiological compartments Equation 3.[16].

$$\begin{aligned}\max_{c,h} \quad & \int_0^\infty e^{-[\rho-(b-d)]t} u(c)dt\\ s.t. \quad & \dot{k} = f(k,1-i) - \delta k - c - h - (b-d)k,\\ & \dot{s} = b - bs - \alpha(h)si + \psi(1-i-s),\\ & \dot{i} = \alpha(h)si - bi - \gamma i.\end{aligned} \tag{5}$$

The control variables are consumption and health expenditure (c,h), and the state variables are (k,i,s). There are alternative ways of solving the optimal con-

[15] Goenka and Liu (2020) have an endogenous growth model where there is human capital accumulation and households choose time to work and time for human capital accumulation. It uses SIS dynamics without disease related mortality.

[16] As the fraction of population in each compartment lies in the simplex The last equation in Equation 3 is redundant by letting $r = 1 - i - s$.

trol problem. If we use the Hamiltonian approach as has been done in most of the literature, the optimal policy in the steady state can be easily computed. However, the optimal policy along a convergence path is difficult to characterize. The issue is that optimal policy in steady state throughout the convergence path causes value loss and the dynamics of the state variables are unknown. In addition, typically for epidemiological model, second order condition do not hold. This was recognized in the first papers (see e.g. Goldman and Lightwood (2002)) but ignored by the literature other than by Goenka, Liu and Nguyen (2014, 2021, 2024). The alternative is to use a continuous time dynamic programming approach that largely circumvents these problems (see e.g. (Achdou et al., 2022; Calvia et al., 2024)). However, to characterize the optimal policy and equilibrium paths, there is the curse of dimensionality.[17] This can be addressed by using neural networks (Fernandez-Villaverde et al., 2020; Fernández-Villaverde, Hurtado and Nuno, 2023). To use this the challenge is which domain to train the neural network in. The most direct way is to globally approximate the value function of the dynamic programming problem, as the universal approximation theorem (Barron, 1993) enable the neural network to approximate any Borel measurable function mapping finite-dimensional spaces to any desired degree of accuracy. The convergence of the approximation is uncorrelated with the number of dimension (Barron, 1993).

In our paper, we apply both approaches. In practice, We firstly pin down the steady state by Hamiltonian Equation 6. $\lambda_1, \lambda_2, \lambda_3$ are the costate variables for the states respectively. μ_1, μ_2, μ_3 are the Lagrangian multipliers for $r > 0, h > 0$. We show the solution strategy for the Hamiltonian in Appendix B.

$$\begin{aligned}\mathcal{H} = \max_{c,h} \quad & e^{-[\rho-(b-d)]t}u(c) + \lambda_1[f(k,1-i) - \delta k - c - h - (b-d)k] \\ & + \lambda_2[b - bs - \alpha(h)si + \psi(1-s-i)] \\ & + \lambda_3[\alpha(h)si - bi - \gamma i] + \mu_1 s + \mu_2 i + \mu_3 h.\end{aligned} \tag{6}$$

For the policy function and the dynamics, we use the dynamic programming approach, which is verified and guild by our analytical solution from Hamiltonian. We target at solving the current value Hamiltonian-Jacobian-Bellman Equation (Equation 7), where $v(k,s,i)$ is the value function. The derivation of HJB is shown in Appendix C.

[17] The coding and computing complexity is exponential to number of state variables. To illustrate this, we take the popular iterated-based algorithm Finite Differencing Method (FDM) (Achdou et al., 2022) as an example. Each state variable has 2 numerical differencing directions (forward, backward). There would be $2^3 = 8$ directions in combined for our (k,i,s) state space ($2^4 = 16$ when we introduce mortality later). Furthermore, suppose each state variable is discretized by (usually) 1000 grids. The FDM needs to invert a $1000^3 \times 1000^3$ matrix.

$$
\begin{aligned}
(\rho - b + d)v(k,s,i) = \max_{c,h} \quad & u(c) + \frac{\partial v}{\partial k}\dot{k} + \frac{\partial v}{\partial i}\dot{i} + \frac{\partial v}{\partial s}\dot{s} \\
= \max_{c,h} \quad & u(c) + \frac{\partial v}{\partial k}[f(k,1-i) - \delta k - c - h - (b-d)k] \\
& + \frac{\partial v}{\partial i}[\alpha(h)si - bi - \gamma i] \\
& + \frac{\partial v}{\partial s}[b - bs - \alpha(h)si + \psi(1-s-i)].
\end{aligned} \tag{7}
$$

The F.O.C. for the HJB reads

$$
\begin{cases}
c: & u'(c) - v_k(k,s,i) = 0 \\
h: & -v_k(k,s,i) + \alpha'(h)si[v_i(k,s,i) - v_s(k,s,i)] = 0,
\end{cases} \tag{8}
$$

which implies that the optimal policy could be expressed as functions of state variables and the marginal value as follow

$$
\begin{cases}
c^* = u'^{-1}(v_k) \\
h^* = \alpha'^{-1}\left(\frac{v_k}{si(v_i - v_s)}\right).
\end{cases} \tag{9}
$$

The expression of the optimal health expenditure h^* is quite intuitive. The inverse function of marginal contact α'^{-1} is feasible only with negative input as the contact function α is assumed to be decreasing. While (v_k, s, i) being positive, the optimal health expenditure requests $v_i < v_s$. This implies that it is optimal to spend positive amount of precautionary expenditure only when the marginal value by one more infected people being smaller than the marginal value by one more susceptible people. When the gap in the marginal values $|v_i - v_s|$ gets wilder, it becomes more beneficial to control the pandemic. The social planner would hence optimally spend more on health.

In our paper, the HJB is approximated by the deep learning neural network normally around the steady state obtained independently by Hamiltonian approach. We demonstrate our neural network algorithm in Appendix D. We found the combination of two approaches boots the efficiency and precision that the paths computed by the neural network indeed converge to the steady state that can be determined theoretically via the Hamiltonian approach.

C. *Parameterization*

The model is calibrated in the quarterly frequency. The birth rate $b = 0.005$ implies 2% of annual birth rate; death rate $d = 0.0031$ implies an 80 years of

life expectancy. For the utility function, we assume CRS preference with $\sigma = 2$, subjective discount rate $\rho = 0.0138$.

$$u(c) = \frac{c^{1-\sigma}}{1-\sigma}. \tag{10}$$

The production function takes the standard C-D form that $f(k, 1-i) = Ak^{\beta}(1-i)^{1-\beta}$ with $\beta = 0.36$; Depreciation rate $\delta = 0.0125$; Technology $A = 3$.

Our parameterization for the epidemiology part of the model follows the discussion by Goenka, Liu and Nguyen (2021, 2024). We assume $\gamma = 9$, which generates 10 days of recovery time from infection.[18] We also calibrate $\psi = 1$ for the SIRS model where the immunity could only last for a quarter; $\psi = 0$ for the SIR model where permanent immunity is assumed. Finally, the contact rate function in our paper takes the form of Equation 11. We parameterize this function to be in line with assumption 2 and large enough to generate endemic steady state. However, we notice that it is hard to find empirical evidence to calibrate the contact function. In our baseline model, we let $\epsilon_0 = 11.03, \epsilon_1 = -0.3, \epsilon_2 = 0.01$, implying that the basic reproduction number without any health expenditure would be 5[19], and the contact rate elasticity of health expenditure converges to -0.3 as h increases.[20]

$$\alpha(h) = \epsilon_0(h + \epsilon_2)^{\epsilon_1}. \tag{11}$$

Under the parameterization above, the Hamiltonian (Equation 6) presents an endemic steady state with $k^{SIRS} = 316, i^{SIRS} = 0.0478, s^{SIRS} = 0.52, h^{SIRS} = 0.23, c^{SIRS} = 18.3$, and $k^{SIR} = 331, i^{SIR} = 0.0004, s^{SIR} = 0.2, h^{SIR} = 0, c^{SIR} = 19.46$. In Appendix B, we vary elasticity parameter ϵ_1 and the reinfection rate ψ in complement to our baseline calibration.

III. Baseline Result

Optimal Health Policy. We now begin presenting the main results of our paper. We firstly show the health policy functions $h(k, s, i)$.[21] We notice that there

[18] See i.e. UK Health Security Agency (2023) shows that most studies report a virus clearance time around 7 to 15 days.

[19] The basic reproduction number in the pure epidemiological model is calculated by the ratio of contact rate with recovery rate, i.e. $R_0 = \frac{\alpha}{b+\gamma}$. In the data, R_0 for the Delta variant is estimated to be around 3.3 to 6.4 (See i.e. the summary by Sepandi, Alimohamadi and Esmaeilzadeh (2022)); for the Omicron variant is estimated to be around 5.5 to 24 (See i.e. summary by Liu and Rocklöv (2022)).

[20] The contact rate elasticity of health expenditure in our contact function would be $\frac{d\alpha}{dh} \times \frac{h}{\alpha} = \frac{\epsilon_1}{1+\frac{\epsilon_2}{h}}$.

[21] Consumption and value function are shown in the appendix Figure A1 and Figure A2. They are decreasing with both s and i. In magnitude, SIR model shows larger consumption and value.

Figure 2. Policy Functions H

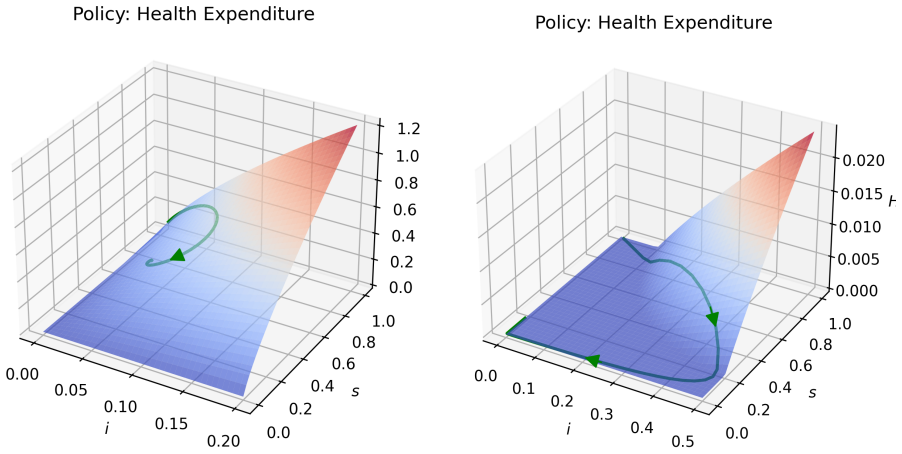

(a) SIRS **(b)** SIR

Notes: (i) Panel (a) and (b) show the optimal health policy function $h^*(k, i, s)$ for SIRS and SIR model. We marginalize the capital at its steady state k^{SS}. (ii) The green solid line with arrows are the simulated convergence paths initialized with $(k_0, i_0, s_0) = (280, 1\%, 99\%)$

is a natural difficulty in visualizing a function with 3 continuous input. Therefore, we marginalize one dimension by holding $k = k^{ss}$ in the main text.

Figure 2 shows the corresponding results. Panel (a) represents the SIRS model where recovered people have temporary immunity. Panel (b) represents the SIR model where immunity is permanent. One can easily observe that the policy functions between different models looks qualitatively similar. The health expenditure is increasing with both susceptible rate (s) and infection rate (i) for both models. However, compared with the SIRS model, the magnitude for SIR model is much smaller, with a large area of 0. This is because for the SIR model, infection brings life-long immunity which migrates part of the loss. Value of controlling the pandemic is not as substantive as that in the SIRS model.

Dynamics. Although the health policy functions for two models look qualitatively similar, they would generate structural differences for the dynamics of state variables. To see this, we assign the initial state with $(k_0, i_0, s_0) = (280, 1\%, 99\%)$ and simulate two models using the corresponding policy functions. Figure 3 shows the generated dynamics of epidemiological states.[22] For the SIRS model in the left, s doesn't reduce too much as the recovered people would lose their immunity and back to the susceptible group. The infection rate i is persistent that people keep getting infected due to a large group of susceptible.

Conversely, for the SIR model in the right Panel, the infection rate peaks at around one month after the outbreak, which comes much earlier than that in the

[22]In the appendix Figure A3, we plot the simulated path for capital and labour participation.

Figure 3. Composition Change for Compartments

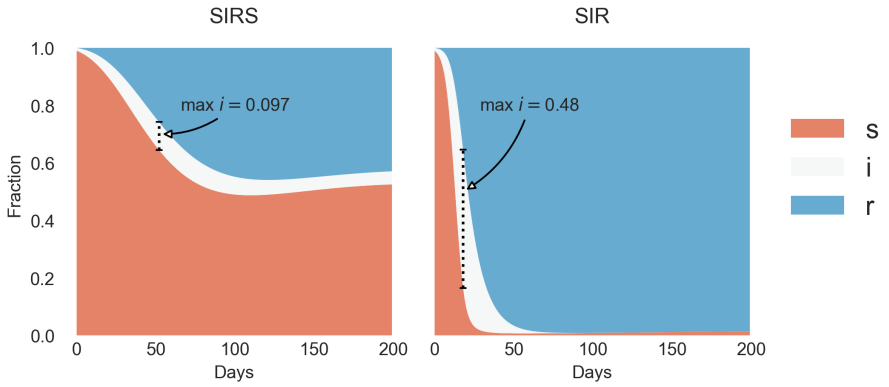

Notes: (i) This is the stack plot for epidemiological compartments in SIRS and SIR model. The red, white and blue area denote the fractions of susceptible, infective and recovered groups respectively. The horizontal axis is the days of simulation. (ii) The little dash bars show the maximum infection rate throughout the simulated periods.

SIRS model. The peak infection rate hits 48% which is also much higher than that of 10% in the SIRS model. However, during the pandemic, the size of susceptible shrinks down very quickly while the recovered group expands. This is because people obtain permanent immunity as they get over the disease. Consequently, the infection rate in the SIR model eventually reduces to very small in the steady state as there are little susceptibles left.

Despite the different magnitudes in the health policy functions, the different motions of state (s, i) also affect the optimal paths for health expenditure h. As shown in the green lines in Figure 2, the ways that h^* moves on the equilibrium surface are not similar to each other. For the SIRS model, the motion of health expenditure h^* moves to the central of the surface, with $h^* > 0$ all the time. For the SIR model, however, the motion moves towards the corner with low infection and susceptible rates, where $h^* = 0$.

To further visualize the dynamics of the model, we now plot the phase diagrams[23] for SIRS and SIR models in Figure 4. The red solid curves separate the regions with different directions of motion. The black dash curves are the paths of our simulated example in Figure 3. The blue area represents the sample density for our neural network approximation. Moreover, as we mentioned before, we solve the steady states of the models analytically by Hamiltonian as validations for our neural network approach. We mark the Hamiltonian solution by the yellow crosses in the Figure. It further validates our neural network approach that the analytical solutions for steady states are sufficiently close to the simulated solutions where two

[23] As complements for the phase diagram, we plot the surface for $(s, i, \dot{s}), (s, i, \dot{i})$ in appendix Figure A5 and Figure A6

Figure 4. Phase Diagram

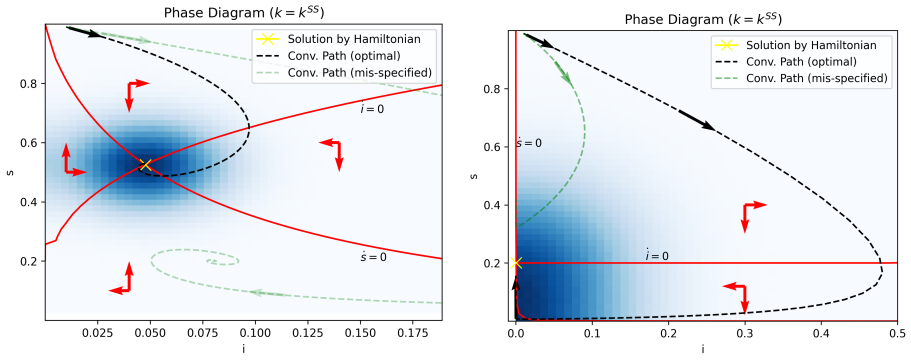

(a) SIRS **(b)** SIR

Notes: (i) This Figure plots the phase diagrams at (s, i) panel for SIRS and SIR model. The other state variable k is marginalized to its steady state. (ii) The red curves represent combinations with s or i being steady. The intersections of two lines are the simulated steady states where both variables remain unchanged. (iii) The yellow crosses are the analytical solutions of steady states obtained by Hamiltonian (Equation 6). (iv) The black dash lines with arrows are the simulated paths for demonstration. (v) The blue area is the density for the combinations used to train the neural network.

red curves join together.

Notice that the dynamics of (s, i) in a pure epidemiological SIRS model, i.e. Hethcote (2000), is a spiral sink as shown in the Appendix Figure A4. The phase diagrams in our model would show a similar pattern — (s, i) evolves following a stable focus dynamics. When it comes to the comparison between different model specifications, we find that the space with increasing motion of susceptible (area with $\dot{s} > 0$) is largely squeezed for the SIR model. Correspondingly, the susceptible size in the SIR model decreases for the most of the time. The second key difference is that the threshold line $\dot{i} = 0$ in the SIRS model is steeper due to a more active health policy. Consequently, there shows a smaller area for infection expansion with $\dot{i} > 0$. Thus, the infection rate in the SIRS model goes through the increasing stage easier and generates a lower peak of infection as we mentioned before.

Misspecified Model. We now discuss the consequence of misspecifying the epidemiological models. We simulate the dynamics given the same initial states but with the misspecified health policy. For example, when the disease follows the SIRS dynamics, we assume that the social planner mistakenly applies the optimal health policy for the SIR model. Practically, we exogenously impose the SIR health policy to the simulation of the SIRS model. Same logic is applied for the case of disease with SIR dynamics. This is to see the counter-factual effect of adopting the optimal policy for the wrong dynamics. This gives an estimate for how much the epidemiological component matters in an economic epidemiology model.

The corresponding paths for the state variables (s, i) with the misspecified model

Figure 5. Value Loss of being Laissez-Faire

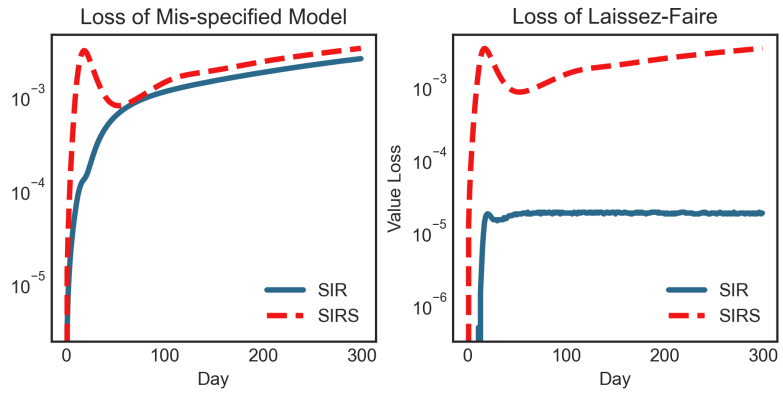

Notes: (i) This Figure plots the value loss under different scenarios. The red and blue curves denote SIRS and SIR models respectively. (ii) The left panel shows the case of model mis-specification that social planner use the health policy from the other model. (iii) The right panel shows the case of Laissez-Faire that social planner does not impose any intervention.

are plot in green dash line in Figure 4. It could be viewed that if the social planner mistakenly imposes the SIR health policy, while SIRS is the actual epidemiology model, the consequential infection rate increases further away from its optimum for both steady state and transitional path. Conversely, if the SIR model is misspecified as the SIRS model, the social planner spends more health expenditure than the optimal level. The increase of infection rate therefore gets milder. However, as we show in the appendix Figure A3, the extra spending in health slows down the capital accumulation. The capital goes eventually below optimum, although the infection rate is effectively controlled.

What is the net loss for misspecifying the epidemiology model? We calculate the value loss, which is defined as the gap between the optimal and counterfactual value functions. Figure 5 shows the corresponding results. We find the loss for misspecifying model is always positive. We would like to mark that the value losses for different models originate from different sources. For the SIRS model, the loss comes from the extra infection that incapacitates more labour. For the SIR model, the loss comes from the extra financial cost of health expenditure.

It can be further noticed that the loss for misspecifying SIRS model is higher than that for misspecifying SIR model, especially at the beginning of the pandemic. Such observation may have deep policy implications for the social planner. When the characteristics of the disease is unknown that misspecification could happen, the maximin strategy[24] for the social planner would be treating the disease using the SIRS model. In a plain word, it would be better-off for the policymaker to control the spread of the disease when it is unclear whether re-infection could take place.

[24] A strategy that maximizes the minimum payoff.

Table I. Pay-off Matrix

	Models	
	SIR	*SIRS*
Controls		
SIR	-0	-0.43
SIRS	-0.055	-0.36
Laissez-Faire	-0.003	-0.44

Notes: For visualizing a tidier table, the elements are the standardized payoff +100

To further discuss this argument, we present a pay-off matrix as Table I. The columns in the matrix denote the actual epidemiology model, while the rows denote the health policy applied. For example, the first element indicates the pay-off when the social planner correctly identify the SIR disease and use the optimal health policy derived from the SIR model. Just for illustration, we use the value at the steady state as the pay-off and standardize the first element to be -100. From the matrix, one can easily show that when the type of model is known, the correctly-specified policy yield higher pay-off. However, when the type is unknown, the minimax strategy in case of the worst situation, i.e. situation when re-infection could take place, would be treating the unknown disease using the SIRS model. Moreover, if we let p to be the probability that the disease follow the SIRS dynamics, we can easily solve out a cut-off value $p^* = 0.43$, above which SIRS strategy is optimal.

IV. Vaccination and Mortality

Vaccination. We model vaccination in a simple way similar to Federico, Ferrari and Torrente (2022). We notice that vaccinated group essentially shares similar characteristics with recovered group. They both carry temporary immunity to disease. The key difference is the way of obtaining immunity. People in recovered group naturally gain immunity by overcoming infection, while vaccination brings susceptible people directly to the immune group without going through infection. Thus, a higher vaccination rate implies more recovered and less susceptible before the pandemic hit the economy. With this property, we could model the effect of vaccination efficiently by altering the size of pre-existing susceptible group. We vary the simplex of initial shares of epidemiological compartments (s_0, i_0) and simulate

Figure 6. Vaccination

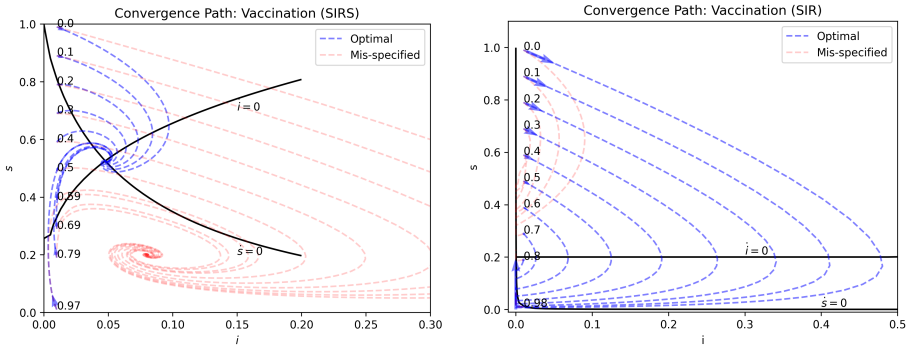

(a) SIRS **(b)** SIR

Notes: (i) This Figure shows the simulated paths with multiple initial values. The numbers at the left edge are the fractions of pre-existing recovery group. We use it as a proxy for vaccinated group. (ii) The blue and red lines are the convergence paths under optimal and Laissez-Faire scenario respectively.

the corresponding paths.[25] We fix the initial infection rate $i_0 = 1\%$ as our previous studies. The initial susceptible s_0 is varied from 3% to 100%. Smaller s_0 implies more pre-existing immunity by higher vaccination rate.

In Figure 6, we plot the simulated paths $\{(s_t, i_t)\}_{t=(0,\infty)}$ with blue dash lines. We mark the share of the vaccinated population at the edges of the paths. It could be seen that all paths converge to the same steady state. However, with a lower rate of vaccination, the economy shows steeper increase and higher peak value of infection rate. In line with the previous section, using the same initial values, we also simulate paths under the scenarios that the model is misspecified, where we assume that the SIR health policy is used. We plot the corresponding results using the red dash line. Compared with the optimal paths, the misspecified paths converge to a different steady state with higher infection but lower susceptible rate. The economy would thus go through worse pandemic. Panel (b) of Figure 6 shows the counterpart using SIR model. We could have similar findings that higher vaccination rate generates lower peak of infection during the outbreak.

Introducing Mortality. In the canonical epidemiological economic models presented above, mortality is absent. The reasons why we abstract mortality in the main part of the paper are two folded. Firstly, the later evidence of Covid-19

[25] Another possible approach is to introduce a new compartment for vaccinated group like e.g. Sun and Yang (2010); Safan, Kretzschmar and Hadeler (2013); Garriga, Manuelli and Sanghi (2022) (another health status in our model). The vaccinated group is mostly similar to the recovered group as they both carries temporary immunity. The only difference is on their reinfection probability. Clinical evidence shows immunity from previous infection lasts longer than from primary series or first booster of vaccination. But the gap is not pronounced (Bobrovitz et al., 2023)

pandemic when Omicron variant dominates shows that the mortality rate is small.[26] The second reason is technical. When introducing disease related mortality into the model, the total population in the economy changes as a function of endogenous state (s, i).[27] This makes the discounting endogenous (Goenka, Liu and Nguyen, 2024). In dynamic programming, the additional state variable due to mortality also makes it even harder for visualizing the policy function and phase diagram as the state space is four-dimensional.

Here, to further or analysis, we augment our model by introducing mortality in the following way.[28] Mortality of the infected from the disease is at the rate of ϕ. This implies that the change of total population satisfies expression $\frac{\dot{N}}{N} = b - d - \phi i$. The social discount rate is hence endogenous as a function of cumulative mortality rate.[29] Specifically, the social planner discount his utility by $e^{-\theta_t}$, where

$$\begin{aligned} \theta_t &= \int_0^t (\rho - b + d + \phi i_\tau) d\tau, \\ \dot{\theta}_t &= \rho - b + d + \phi i_\tau. \end{aligned} \tag{12}$$

We additionally adopt the assumption of non-pecuniary punishment of disease-induced mortality. That is, we directly deduct the loss of mortality from the utility function.[30] Let the relative loss to social welfare from mortality be $\chi(\phi i)$ and it satisfies $\chi'(\cdot) > 0, \chi''(\cdot) \geq 0$. The utility function for the social planner becomes $u(c) - \chi(\phi i)$. In parameterization, we set $\phi = 0.5\%$ in our paper, in lined with Sorensen et al. (2022)'s estimation for 39 countries that the Infection Fatality Ratio (IFR) to be around 0.233% - 0.84% at 2020, and around 0.314% - 0.551% at 2021. For the functional form of $\chi(z)$, we follow Goenka, Liu and Nguyen (2024) to assume a linear non-pecuniary punishment that $\chi(z) = \xi z$. The value of χ is linked with the Value of Statistical Life (VSL).[31] We vary parameter ξ in 1.028, 3.77 and 6.42, corresponding to the steady-state VSL of 1, 40 and 80 times of production per capita. This is in lined with Alvarez, Argente and Lippi (2021) where the benchmark VSL is 40 times of GDP per capita.

We follow the same strategy as section II. for analysing the model. To solve the

[26] UK data shows around 100 or less of daily numbers of deaths of people whose death certificate mentioned COVID-19 as one of the causes.

[27] As a preview of the result, in Appendix Figure A9, we plot the change of compartment composition as in Figure 3. It could be seen that the total population is decreasing with time due to the extra mortality by disease.

[28] We show the flow chart for the extended model in appendix Figure A7

[29] See e.g. Goenka, Liu and Nguyen (2024).

[30] See e.g. the discussion in Acemoglu et al. (2021); Boucekkine et al. (2024); Goenka, Liu and Nguyen (2024) etc..

[31] VSL is the value of increasing the survival probabilities marginally (Acemoglu et al., 2021). We follow Andersson and Treich (2011) to obtain the VSL at steady state by $\Delta y / \Delta \phi i$ while there is concave utility in the objective function.

steady state as the first step, we specify the Hamiltonian as Equation 13. Then, we study the dynamics of the model by solving HJB Equation 14. We show the process of solving Hamiltonian and specifying HJB in Appendix B and Appendix C.

$$\begin{aligned}\mathcal{H} = \max_{c,h} \quad & e^{-\theta}[u(c) - \chi(\phi i)] \\ & + \lambda_1 \{f(k, 1-i) - \delta k - c - h - (b - d - \phi i)k\} \\ & + \lambda_2 \{b - bs - \alpha(h)si + \psi(1 - s - i) + \phi si\} \\ & + \lambda_3 \left\{\alpha(h)si - bi - \gamma i - \phi i + \phi i^2\right\} \\ & + \lambda_4 \{r - b + d + \phi i\} + \mu_1 s + \mu_2 i + \mu_3 h.\end{aligned} \tag{13}$$

$$\dot{\theta} V(k, i, s, \theta) = \sup_{c,h} \left\{ u(c) - \chi(\phi i) + \frac{\partial V}{\partial k}\dot{k} + \frac{\partial V}{\partial i}\dot{i} + \frac{\partial V}{\partial s}\dot{s} + \frac{\partial V}{\partial \theta}\dot{\theta} \right\}. \tag{14}$$

Figure 7 shows the convergence path with different calibrations of parameter ξ in the non-pecuniary punishment function. For comparison, we also plot the convergence paths of the baseline SIRS model in the gray dash lines. We find the basic structure of the dynamics looks similar for models with or without mortality. The health policy is pro-cyclical to the social infection rate. The convergence paths of capital and consumption are negatively affected by pandemic during the first 100 days. The labour is also dampened during the pandemic and recover back to its steady state, which is smaller than the initial value. Differently, we find that the steady labour is smaller than our baseline model.

The paths also show some counter-intuitive results. We find that for the calibration with lower mortality punishment, i.e. VSL equals output (blue lines) and VSL equals 40 times of output (red lines), the optimal health expenditure is smaller than the standard SIRS model without mortality. The corresponding infection rate is thus higher.

We provide a possible explanation on why mortality oppositely reduces optimal health expenditure in the following way. The excess death by the pandemic decreases the total population, which implies that each person could share more capital. The social benefit of holding more capital could overweight the loss by higher infection. This could be roughly shown by the simulation with $VSL = 40y$ (red lines) in Figure 7. The infection rate under this calibration is slightly higher than that in the baseline. However, higher infection doesn't imply lower capital as we anticipate. We find the reduction in capital is not as much as that in the baseline during the first few months. Moreover, when we further increase the direct punishment, i.e. $VSL = 80y$ (green lines), the optimal health expenditure becomes strictly higher than the baseline. There is another epidemiological reason why mortality has this counter-intuitive effect. Higher mortality reduces the number of infective individuals

Figure 7. Convergence Path for SIRS model with Mortality

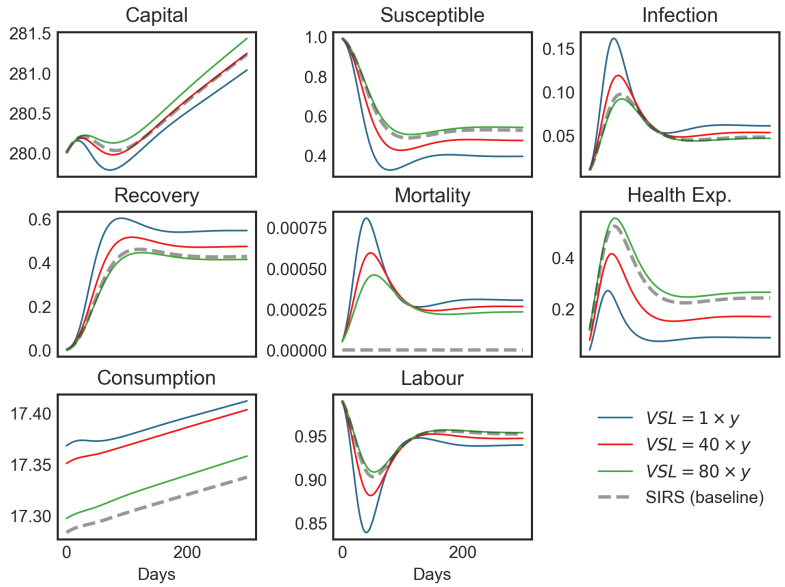

Notes: (i) This Figure shows the convergence paths under different levels of direct punishment on mortality. (ii) The gray dash lines are the referenced paths in our baseline SIRS model without mortality and Long Covid.

reducing the transmission of the disease. That is, mortality has a self-limiting effect on the transmission of the disease. Without further useful insights, we plot the transitional paths of the SIR model with mortality in Appendix Figure A8.

V. Conclusion

Our paper computes value and policy functions in the canonical epidemiological economic models by using the deep-learning dynamic programming approach. We visualize and compare the policy functions for health expenditure and the dynamics for two basic epidemiological models (SIR and SIRS models). We conclude with the following remarks: (1) The optimal health policy under SIR and SIRS looks qualitatively similar that it increases with both susceptible and infection rates. The magnitude and dynamics for health policy are different for two models. The optimal health expenditure is larger and persistent under SIRS model. However, for SIR model, health expenditure is smaller during pandemic and is 0 at the steady state. (2) The epidemiological states follows the stable focus dynamics. For SIR, the outbreak of infection is more severe but the stable rate is low. For SIRS, reinfection induces higher infection rate at the steady state. However, the outbreak is milder because of the intervention of health expenditure. (3) If the model is misspecified that the social planner uses the health policy function in the other model, value loss would be induced. The loss of misspecifying SIRS model is larger than that of

misspecifying SIR model. Thus, the social planner could be better-off by treating the disease by SIRS model when disease characteristics are unknown. (4) For vaccination, we show that a higher weight of vaccinated people could efficiently milden the peak infection rate. (5) When we introduce mortality and Long Covid into the model, the optimal path for health expenditure does not necessarily increase as people could share more capital per capita when there is less population. It depends on the contest between the value of statistical life and the gain by holding more capital per capita.

References

Acemoglu, Daron, Victor Chernozhukov, Iván Werning, and Michael D Whinston. 2021. "Optimal targeted lockdowns in a multigroup SIR model." American Economic Review: Insights, 3(4): 487–502.

Achdou, Yves, Jiequn Han, Jean-Michel Lasry, Pierre-Louis Lions, and Benjamin Moll. 2022. "Income and wealth distribution in macroeconomics: A continuous-time approach." The review of economic studies, 89(1): 45–86.

Alvarez, Fernando, David Argente, and Francesco Lippi. 2021. "A simple planning problem for COVID-19 lock-down, testing, and tracing." American Economic Review: Insights, 3(3): 367–382.

Andersson, Henrik, and Nicolas Treich. 2011. "The value of a statistical life." In A handbook of transport economics. Edward Elgar Publishing.

Barron, Andrew R. 1993. "Universal approximation bounds for superpositions of a sigmoidal function." IEEE Transactions on Information theory, 39(3): 930–945.

Bobrovitz, Niklas, Harriet Ware, Xiaomeng Ma, Zihan Li, Reza Hosseini, Christian Cao, Anabel Selemon, Mairead Whelan, Zahra Premji, Hanane Issa, et al. 2023. "Protective effectiveness of previous SARS-CoV-2 infection and hybrid immunity against the omicron variant and severe disease: a systematic review and meta-regression." The Lancet Infectious Diseases.

Boucekkine, Raouf, Shankha Chakraborty, Aditya Goenka, and Lin Liu. 2024. "Economic epidemiological modelling: A progress report." Journal of Mathematical Economics, 103011.

Cagigi, Alberto, Meng Yu, Björn Österberg, Julia Svensson, Sara Falck-Jones, Sindhu Vangeti, Eric Åhlberg, Lida Azizmohammadi, Anna

Warnqvist, Ryan Falck-Jones, et al. 2021. "Airway antibodies emerge according to COVID-19 severity and wane rapidly but reappear after SARS-CoV-2 vaccination." JCI insight, 6(22).

Calvia, Alessandro, Fausto Gozzi, Francesco Lippi, and Giovanni Zanco. 2024. "A simple planning problem for COVID-19 lockdown: a dynamic programming approach." Economic Theory, 77(1): 169–196.

Cele, Sandile, Inbal Gazy, Laurelle Jackson, Shi-Hsia Hwa, Houriiyah Tegally, Gila Lustig, Jennifer Giandhari, Sureshnee Pillay, Eduan Wilkinson, Yeshnee Naidoo, et al. 2021. "Escape of SARS-CoV-2 501Y. V2 from neutralization by convalescent plasma." Nature, 593(7857): 142–146.

Eichenbaum, Martin S, Sergio Rebelo, and Mathias Trabandt. 2021. "The macroeconomics of epidemics." The Review of Financial Studies, 34(11): 5149–5187.

Federico, Salvatore, Giorgio Ferrari, and Maria-Laura Torrente. 2022. "Optimal vaccination in a SIRS epidemic model." Economic Theory, 1–26.

Ferguson, Neil, Daniel Laydon, Gemma Nedjati Gilani, Natsuko Imai, Kylie Ainslie, Marc Baguelin, Sangeeta Bhatia, Adhiratha Boonyasiri, ZULMA Cucunuba Perez, Gina Cuomo-Dannenburg, et al. 2020. "Report 9: Impact of non-pharmaceutical interventions (NPIs) to reduce COVID19 mortality and healthcare demand."

Fernandez-Villaverde, Jesus, Galo Nuno, George Sorg-Langhans, and Maximilian Vogler. 2020. "Solving high-dimensional dynamic programming problems using deep learning." Unpublished working paper.

Fernández-Villaverde, Jesús, Samuel Hurtado, and Galo Nuno. 2023. "Financial frictions and the wealth distribution." Econometrica, 91(3): 869–901.

Flaxman, Seth, Swapnil Mishra, Axel Gandy, H Juliette T Unwin, Thomas A Mellan, Helen Coupland, Charles Whittaker, Harrison Zhu, Tresnia Berah, Jeffrey W Eaton, et al. 2020. "Estimating the effects of non-pharmaceutical interventions on COVID-19 in Europe." Nature, 584(7820): 257–261.

Garriga, Carlos, Rody Manuelli, and Siddhartha Sanghi. 2022. "Optimal management of an epidemic: Lockdown, vaccine and value of life." Journal of Economic Dynamics and Control, 140: 104351.

Goenka, A, and L Liu. 2020. "Human capital, infectious diseases and economic growth." Economic Theory, 70(1).

Goenka, Aditya, and Lin Liu. 2012. "Infectious diseases and endogenous fluctuations." Economic Theory, 50: 125–149.

Goenka, Aditya, Lin Liu, and Manh-Hung Nguyen. 2014. "Infectious diseases and economic growth." Journal of Mathematical Economics, 50: 34–53.

Goenka, Aditya, Lin Liu, and Manh-Hung Nguyen. 2021. "SIR economic epidemiological models with disease induced mortality." Journal of Mathematical Economics, 93: 102476.

Goenka, Aditya, Lin Liu, and Manh-Hung Nguyen. 2024. "Modelling optimal lockdowns with waning immunity." Economic theory, 77(1): 197–234.

Goldman, Steven, and James Lightwood. 2002. "Cost optimization in the SIS model of infectious disease with treatment." Topics in Economic Analysis & Policy, 2(1): 1007.

Hansen, Christian Holm, Daniela Michlmayr, Sophie Madeleine Gubbels, Kåre Mølbak, and Steen Ethelberg. 2021. "Assessment of protection against reinfection with SARS-CoV-2 among 4 million PCR-tested individuals in Denmark in 2020: a population-level observational study." The lancet, 397(10280): 1204–1212.

Hethcote, Herbert W. 2000. "The mathematics of infectious diseases." SIAM review, 42(4): 599–653.

Linka, Kevin, Mathias Peirlinck, and Ellen Kuhl. 2020. "The reproduction number of COVID-19 and its correlation with public health interventions." Computational mechanics, 66: 1035–1050.

Liu, Ying, and Joacim Rocklöv. 2022. "The effective reproductive number of the Omicron variant of SARS-CoV-2 is several times relative to Delta." Journal of travel medicine, 29(3): taac037.

Marini, John J, and Luciano Gattinoni. 2020. "Management of COVID-19 respiratory distress." Jama, 323(22): 2329–2330.

ONS. 2023. "More information on data sources related to coronavirus (COVID-19)."

Sabino, Ester C, Lewis F Buss, Maria PS Carvalho, Carlos A Prete, Myuki AE Crispim, Nelson A Fraiji, Rafael HM Pereira, Kris V

Parag, Pedro da Silva Peixoto, Moritz UG Kraemer, et al. 2021. "Resurgence of COVID-19 in Manaus, Brazil, despite high seroprevalence." The Lancet, 397(10273): 452–455.

Safan, Muntaser, Mirjam Kretzschmar, and Karl P Hadeler. 2013. "Vaccination based control of infections in SIRS models with reinfection: special reference to pertussis." Journal of mathematical biology, 67: 1083–1110.

Sepandi, Mojtaba, Yousef Alimohamadi, and Firooz Esmaeilzadeh. 2022. "Estimate of the basic reproduction number for delta variant of sars-cov-2: a systematic review and meta-analysis." Journal of Biostatistics and Epidemiology.

Sorensen, RJD, RM Barber, DM Pigott, Austin Carter, CN Spencer, SM Ostroff, RC Reiner, Cristiana Abbafati, Christopher Adolph, Adrien Allorant, et al. 2022. "Variation in the COVID-19 infection-fatality ratio by age, time, and geography during the pre-vaccine era: A systematic analysis." The Lancet, 399(10334): 1469–1488.

Sun, Chengjun, and Wei Yang. 2010. "Global results for an SIRS model with vaccination and isolation." Nonlinear Analysis: Real World Applications, 11(5): 4223–4237.

UK Health Security Agency. 2023. "COVID-19 Omicron variant infectious period and transmission from people with asymptomatic compared with symptomatic infection: a rapid review."

Uzawa, Hirofumi. 2017. "Time preference, the consumption function, and optimum asset holdings." In Value, capital and Growth. 485–504. Routledge.

Appendices

A Figures

Figure A1. Consumption Policy Functions

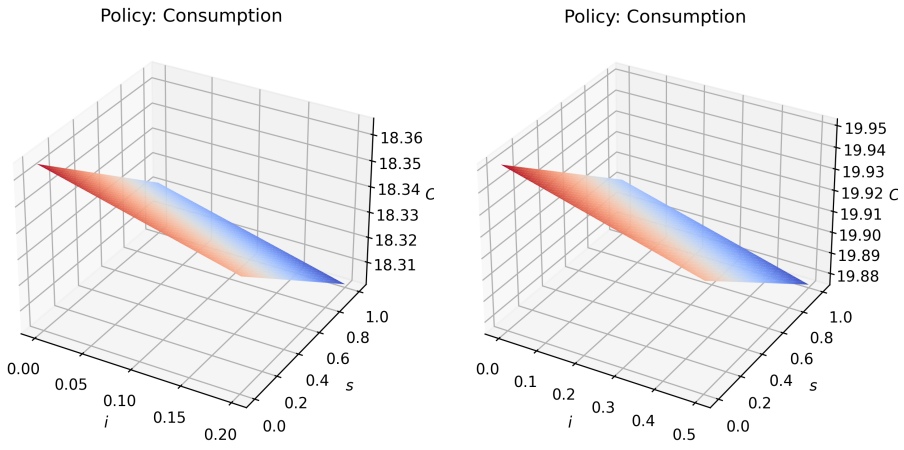

(a) SIRS **(b)** SIR

Figure A2. Value Functions

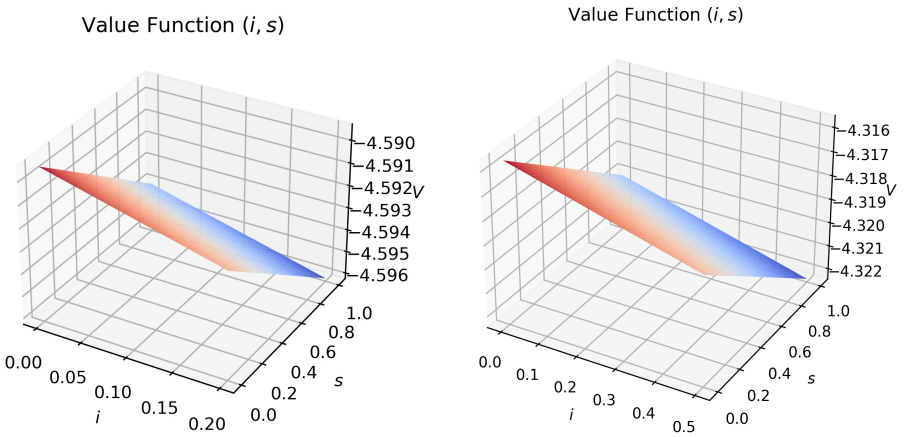

(a) SIRS **(b)** SIR

Figure A3. Path of Capital and Labour Participation

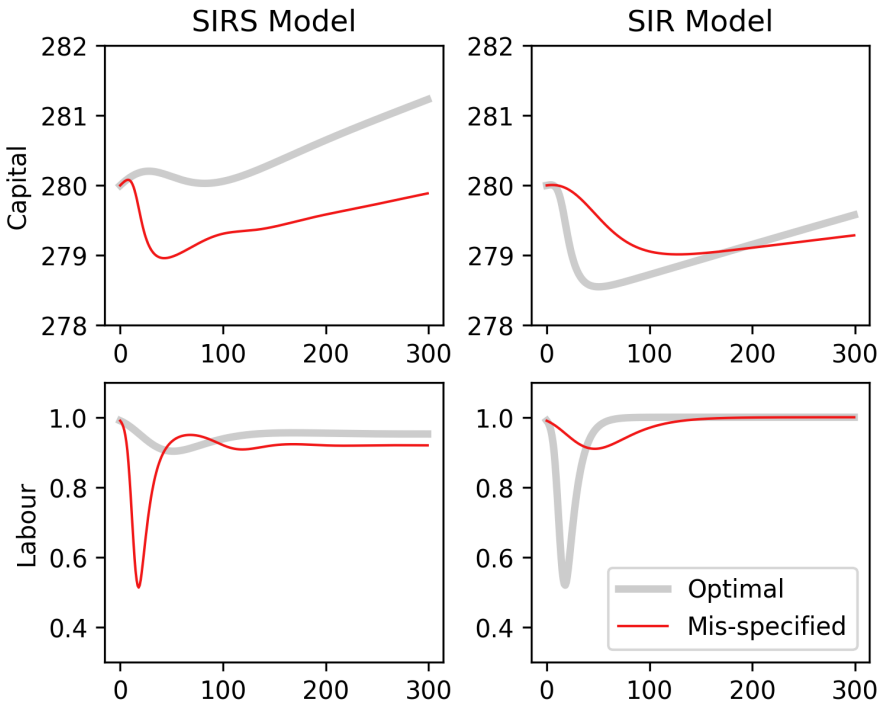

Figure A4. Pure SIRS

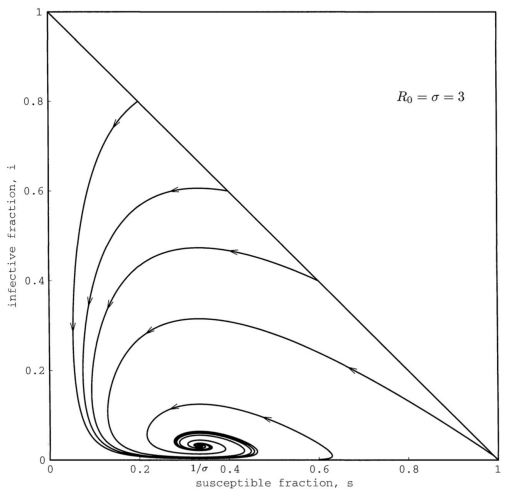

Figure A5. $\dot{i}$ for SIRS and SIR Models

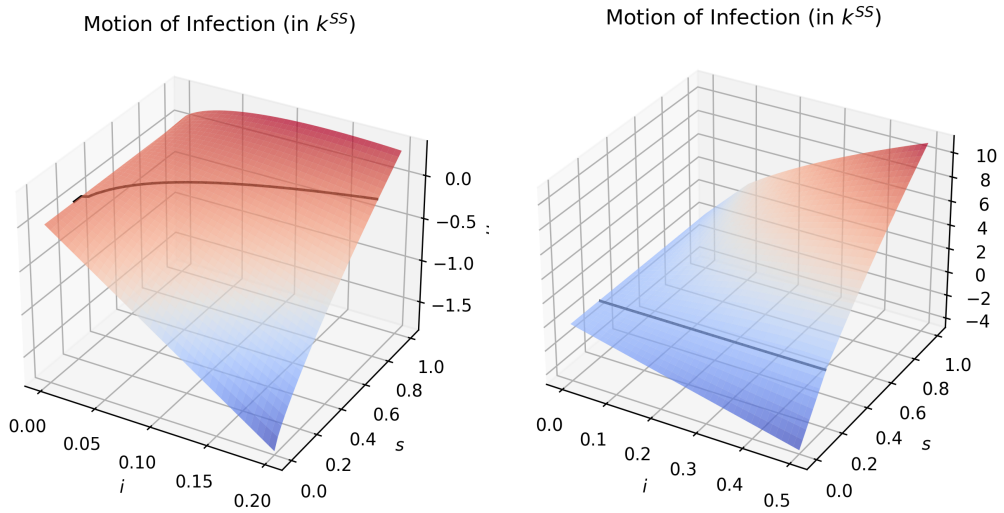

(a) SIRS **(b)** SIR

Figure A6. $\dot{s}$ for SIRS and SIR Models

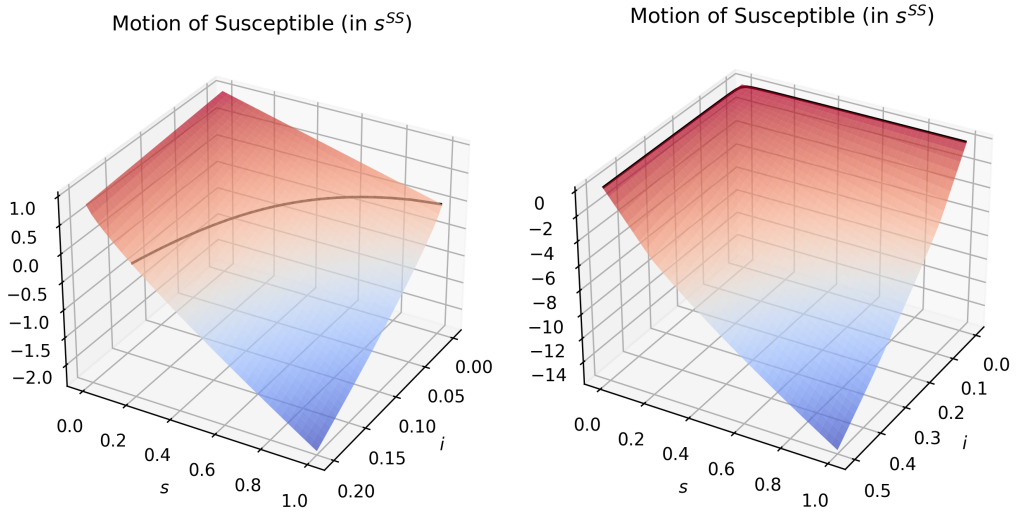

(a) SIRS **(b)** SIR

Figure A8. Convergence Path for SIR model with Mortality

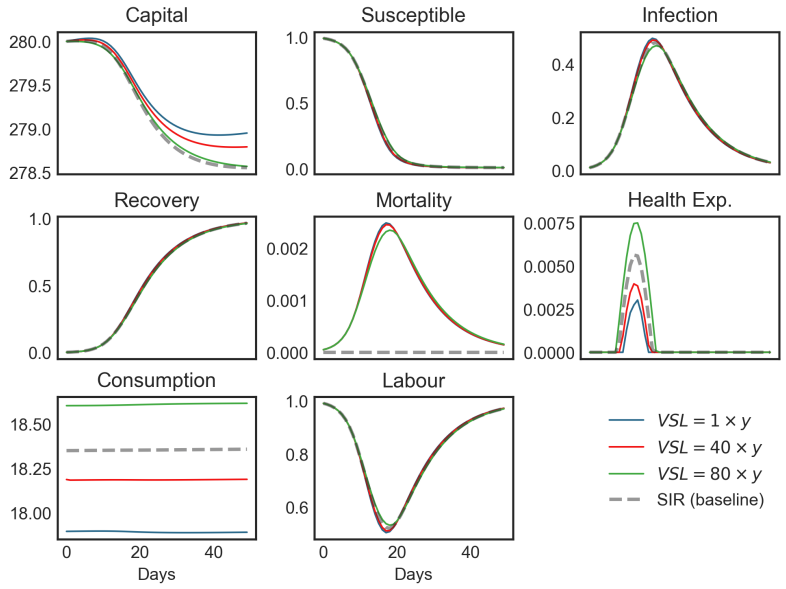

Figure A7. Flow of Epidemiological Compartments

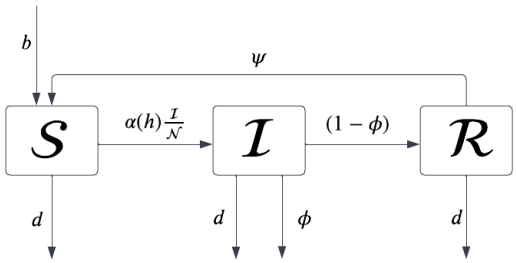

Figure A9. Composition Change for Compartments (Models with Mortality)

B Hamiltonian

A. Baseline SIRS/SIR Model

$$\begin{aligned}
\max_{c,h} \quad & \int_0^\infty e^{-\rho t} u(c) N_0 dt \\
s.t. \quad & \dot{k} = F(k, 1-i) - \delta k - c - h - (b-d)k, \\
& \dot{s} = b - bs - \alpha(h)si + \psi(1-s-i), \\
& \dot{i} = \alpha(h)si - bi - \gamma i, \\
& s \geq 0, \\
& i \geq 0, \\
& h \geq 0,
\end{aligned} \tag{A1}$$

where $\rho = r - (b-d)$. For simplicity, let the initial population $N_0 = 1$, the present value Hamiltonian is

$$\begin{aligned}
\mathcal{H} = \max_{c,h} \quad & e^{-\rho t} u(c) + \lambda_1 [F(k, 1-i) - \delta k - c - h - (b-d)k] \\
& + \lambda_2 [b - bs - \alpha(h)si + \psi(1-s-i)] \\
& + \lambda_3 [\alpha(h)si - bi - \gamma i] + \mu_1 s + \mu_2 i + \mu_3 h.
\end{aligned} \tag{A2}$$

Disease Free Steady State

By Goenka, Liu and Nguyen (2021), there exist disease-free steady state. The disease-free steady state is stable when the contact number

$$\frac{\alpha(0)}{b+\gamma} \leq 1. \tag{A3}$$

The disease-free steady state is determined by

$$\begin{aligned}
& f_1(k, 1) = r + \delta, \\
& c = f(k, 1) - \delta k - (b-d)k.
\end{aligned} \tag{A4}$$

Endemic Steady State

If $\frac{\alpha(0)}{b+\gamma} > 1$, the disease-free steady state is unstable, while the endemic steady state is stable.

The optimal health expenditure h^* is determined by the $G(h)$ function.

Given the endemic steady state, we have $\mu_1 = \mu_2 = 0$. The F.O.C. are

$$
\begin{aligned}
c: &\quad e^{-\rho t}u'(c) - \lambda_1 = 0, && \text{(A5)}\\
h: &\quad -\lambda_1 - \lambda_2\alpha'(h)si + \lambda_3\alpha'(h)si + \mu_3 = 0, && \text{(A6)}\\
k: &\quad -\dot{\lambda_1} = \lambda_1[F_1 - \delta - (b-d)], && \text{(A7)}\\
s: &\quad -\dot{\lambda_2} = \lambda_2[-b - \alpha(h)i - \psi] + \lambda_3\alpha(h)i, && \text{(A8)}\\
i: &\quad -\dot{\lambda_3} = -\lambda_1 F_2 + \lambda_2[-\alpha(h)s - \psi] + \lambda_3[\alpha(h)s - b - \gamma]. && \text{(A9)}
\end{aligned}
$$

By the Equation A5 and Equation A6, we have

$$\mu_3 = \lambda_1 - (\lambda_3 - \lambda_2)\alpha'(h)si. \tag{A10}$$

- $\mu_3 > 0 \Rightarrow MC > MR \Rightarrow h = 0$,
- $\mu_3 = 0 \Rightarrow MC > MR \Rightarrow h > 0$,
- We just need to pin down λ_3, λ_2 and c.

In steady state, we have $\frac{\dot{\lambda}_1}{\lambda_1} = \frac{\dot{\lambda}_2}{\lambda_2} = \frac{\dot{\lambda}_3}{\lambda_3} = -\rho$. From F.O.C.s we have

$$
\begin{aligned}
& -\frac{\dot{\lambda}_2}{\lambda_2} = -b - \alpha(h)i - \psi + \frac{\lambda_3}{\lambda_2}\alpha(h)i = \rho\\
\Rightarrow \quad & \lambda_3\alpha(h)i = [\rho + b + \alpha(h)i + \psi]\lambda_2.
\end{aligned} \tag{A11}
$$

From Equation A9 we have

$$
\begin{aligned}
& -\frac{\dot{\lambda}_3}{\lambda_3} = -\frac{\lambda_1}{\lambda_3}F_2 + \frac{\lambda_2}{\lambda_3}[-\alpha(h)s - \psi] + [\alpha(h)s - b - \gamma] = \rho\\
\Rightarrow \quad & -\lambda_1 F_2 + [\alpha(h)s - b - \gamma - \rho]\lambda_3 = \lambda_2[\alpha(h)s + \psi]\\
\Rightarrow \quad & -e^{-\rho t}u'(c)F_2 + [\alpha(h)s - b - \gamma - \rho]\lambda_3 = \lambda_2[\alpha(h)s + \psi].
\end{aligned} \tag{A12}
$$

Hence, by

$$
\begin{cases}
\lambda_3\alpha(h)i = [\rho + b + \alpha(h)i + \psi]\lambda_2\\
-e^{-\rho t}u'(c)F_2 + [\alpha(h)s - b - \gamma - \rho]\lambda_3 = \lambda_2[\alpha(h)s + \psi].
\end{cases} \tag{A13}
$$

We can solve out

$$
\begin{cases}
\lambda_2 = \frac{e^{-\rho t}u'(c)F_2}{M}\\
\lambda_3 = \left[\frac{\rho + b + \alpha(h)i + \psi}{\alpha(h)i}\right]\lambda_2,
\end{cases} \tag{A14}
$$

where

$$M = \frac{[\alpha(h)s - b - \gamma - \rho][\rho + b + \alpha(h)i + \psi]}{\alpha(h)i} - \alpha(h)s - \psi. \tag{A15}$$

Define $\tilde{\lambda}_1 = \frac{1}{e^{-\rho t}}\lambda_1$, $\tilde{\lambda}_2 = \frac{1}{e^{-\rho t}}\lambda_2$, $\tilde{\lambda}_3 = \frac{1}{e^{-\rho t}}\lambda_3$. So we have

$$\begin{cases} \tilde{\lambda}_2 = \frac{u'(c)F_2}{M} \\ \tilde{\lambda}_3 = \left[\frac{\rho+b+\alpha(h)i+\psi}{\alpha(h)i}\right]\tilde{\lambda}_2. \end{cases} \tag{A16}$$

Then, we can have

$$\begin{aligned} \frac{\mu_3}{e^{-\rho t}} &= \tilde{\lambda}_1 - (\tilde{\lambda}_3 - \tilde{\lambda}_2)\alpha'(h)si \\ &= u'(c) - \left[\frac{\rho + b + \alpha(h)i + \psi}{\alpha(h)i} - 1\right]\frac{u'(c)F_2}{M}\alpha'(h)si \\ &= u'(c) - \left[\frac{\rho + b + \psi}{\alpha(h)i}\right]\frac{u'(c)F_2\alpha'(h)si}{M} \\ &= u'(c)\left[1 - \frac{(\rho + b + \psi)F_2\alpha'(h)s}{\alpha(h)M}\right]. \end{aligned} \tag{A17}$$

Define the G function as

$$G(h) = 1 - \frac{(\rho + b + \psi)F_2\alpha'(h)s}{\alpha(h)M}. \tag{A18}$$

The solution for the optimization problem is determined by the following equations

$$s = \frac{b + \gamma}{\alpha(h)}, \tag{A19}$$

$$i = \frac{b - bs + \psi(1 - s)}{\alpha(h)s + \psi}, \tag{A20}$$

$$f(k, 1 - i) - \delta k - c - h - (b - d)k = 0, \tag{A21}$$

$$f_1(k, 1 - i) = r + \delta, \tag{A22}$$

$$\mu_3 h = 0. \tag{A23}$$

Solution Strategy:

- From the first 2 expression, we can have i, s as function of h. i.e. $\hat{i}(h), \hat{s}(h)$.
- From the forth equation $f(k, 1 - \hat{i}(h))$, we can solve out k as a function of h. i.e. $\hat{k}(h)$.
- Calculate $G(0)$.
  - If $G(0) > 0$, Corner Solution, the we have $h^* = 0$.

– If $G(0) < 0$, Interior Solution, the solution of h^* is given by $G(h) = 0$.

Figure A10. G Function

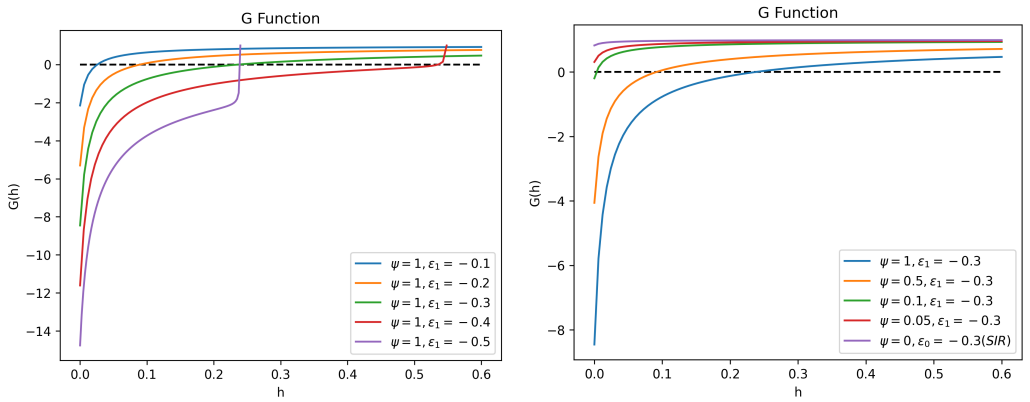

(a) Varying ϵ_1 **(b)** Varying ψ

B. SIRS Model with Mortality and Long Covid

We focus on the endemic steady state. For generalization, we draw further assumption that the recovered people are also faced with η fraction of productivity loss. This assumption could be used to model Long Covid. The Hamiltonian for the optimization problem is

$$\begin{aligned}\mathcal{H} = \max_{c,h} \quad & e^{-\Theta}[u(c) - \chi(\phi i)] \\ & + \lambda_1 \{f(k, 1 - i - \eta(1 - s - i)) - \delta k - c - h - (b - d - \phi i)k\} \\ & + \lambda_2 \{b - bs - \alpha(h)si + \psi(1 - s - i) + \phi si\} \\ & + \lambda_3 \{\alpha(h)si - bi - \gamma i - \phi i + \phi i^2\} \\ & + \lambda_4 \{r - b + d + \phi i\} + \mu_1 s + \mu_2 i + \mu_3 h.\end{aligned} \tag{A24}$$

The F.O.C.s are

$$
\begin{aligned}
c: \quad & e^{-\Theta}u'(c) - \lambda_1 = 0, && \text{(A25)}\\
h: \quad & -\lambda_1 - \lambda_2\alpha'(h)si + \lambda_3\alpha'(h)si + \mu_3 = 0, && \text{(A26)}\\
k: \quad & -\dot{\lambda}_1 = \lambda_1(f_1 - \delta - b + d + \phi i), && \text{(A27)}\\
s: \quad & -\dot{\lambda}_2 = \lambda_1 f_2\eta + \lambda_2[-b - \alpha(h)i - \psi + \phi i] + \lambda_3\alpha(h)i + \mu_1, && \text{(A28)}\\
i: \quad & -\dot{\lambda}_3 = -e^{-\Theta}\chi'(\phi i)\phi + \lambda_1[f_2(\eta - 1) + \phi k] + \lambda_2[-\alpha(h)s - \psi + \phi s] && \text{(A29)}\\
& + \lambda_3[\alpha(h)s - b - \gamma - \phi + 2\phi i] + \lambda_4\phi + \mu_2, && \text{(A30)}\\
\Theta: \quad & -\dot{\lambda}_4 = -e^{-\Theta}[u(c) - \chi(\phi i)]. && \text{(A31)}
\end{aligned}
$$

From the Equation A27, we have

$$
\begin{aligned}
-\frac{\dot{\lambda}_1}{\lambda_1} &= f_1 - \delta - b + d + \phi i\\
&= f_1 - \delta - b + d + \phi i.
\end{aligned}
\tag{A32}
$$

From F.O.C.c we have

$$
\begin{aligned}
\frac{\dot{\lambda}_1}{\lambda_1} &= -\dot{\Theta} + \frac{u''(c)}{u'(c)}\dot{c}\\
&= -(r - b + d + \phi i) + \frac{u''(c)}{u'(c)}\dot{c}
\end{aligned}
\tag{A33}
$$

Using $\dot{c} = 0$ in steady state, we have

$$
\frac{\dot{\lambda}_1}{\lambda_1} = -(r - b + d + \phi i). \tag{A34}
$$

Therefore, we have $f_1 = r + \delta$.
Then, using condition that growth rate for co-states are the same

$$
\frac{\dot{\lambda}_1}{\lambda_1} = \frac{\dot{\lambda}_2}{\lambda_2} = \frac{\dot{\lambda}_3}{\lambda_3} = \frac{\dot{\lambda}_4}{\lambda_4} = -(r - b + d + \phi i) \equiv g. \tag{A35}
$$

Equation A28 yields

$$
\begin{aligned}
-g\lambda_2 &= \lambda_1 f_2\eta + \lambda_2[-b - \alpha(h)i - \psi + \phi i] + \lambda_3\alpha(h)i\\
[-g + b + \alpha(h)i + \psi - \phi i]\lambda_2 - \lambda_3\alpha(h)i &= \lambda_1 f_2\eta\\
[r + d + \psi + \alpha(h)i]\lambda_2 - \lambda_3\alpha(h)i &= \lambda_1 f_2\eta\\
[r + d + \psi + \alpha(h)i]\tilde{\lambda}_2 - \alpha(h)i\tilde{\lambda}_3 &= f_2\eta\tilde{\lambda}_1.
\end{aligned}
\tag{A36}
$$

where we let $\tilde{\lambda}_j = \frac{\lambda_j}{e^{-\Theta}}$

Similarly, Equation A30 yields

$$\begin{aligned}[-g-\alpha(h)s+b+\gamma+\phi-2\phi i]\lambda_3 &= -e^{-\Theta}\chi'(\phi i)\phi+\lambda_1[f_2(\eta-1)+\phi k]+\lambda_2[-\alpha(h)s-\psi+\phi s]+\lambda_4\phi\\ [r+d-\phi i-\alpha(h)s+\gamma+\phi]\lambda_3 &= -e^{-\Theta}\chi'(\phi i)\phi+e^{-\Theta}u'(c)[f_2(\eta-1)+\phi k]+\lambda_2[-\alpha(h)s-\psi+\phi s]\\ &\quad+\frac{e^{-\Theta}[u(c)-\chi(\phi i)]}{-(r-b+d+\phi i)}\phi.\end{aligned} \tag{A37}$$

That is

$$[\alpha(h)s+\psi-\phi s]\tilde{\lambda}_2+[r+d-\phi i-\alpha(h)s+\gamma+\phi]\tilde{\lambda}_3 = -\chi'(\phi i)\phi+u'(c)[f_2(\eta-1)+\phi k]-\frac{u(c)-\chi(\phi i)}{r-b+d+\phi i}\phi. \tag{A38}$$

Then, we can solve out $\tilde{\lambda}_2, \tilde{\lambda}_3$ unitedly by

$$\begin{cases}[r+d+\psi+\alpha(h)i]\tilde{\lambda}_2-\alpha(h)i\tilde{\lambda}_3 = f_2\eta u'(c)\\ [\alpha(h)s+\psi-\phi s]\tilde{\lambda}_2+[r+d-\phi i-\alpha(h)s+\gamma+\phi]\tilde{\lambda}_3 = -\chi'(\phi i)\phi+u'(c)[f_2(\eta-1)+\phi k]-\frac{u(c)-\chi(\phi i)}{r-b+d+\phi i}\phi.\end{cases} \tag{A39}$$

Notate the coefficients for $\tilde{\lambda}_2$ and $\tilde{\lambda}_3$ we have

$$\begin{cases}w_{11}\tilde{\lambda}_2+w_{12}\tilde{\lambda}_3 = I_1\\ w_{21}\tilde{\lambda}_2+w_{22}\tilde{\lambda}_3 = I_2.\end{cases} \tag{A40}$$

From Equation A26 we have

$$\begin{aligned}\mu_3 &= \lambda_1+\lambda_2\alpha'(h)si-\lambda_3\alpha'(h)si\\ &= e^{-\Theta}u'(c)+(\lambda_2-\lambda_3)\alpha'(h)si\\ &= e^{-\Theta}[u'(c)+(\tilde{\lambda}_2-\tilde{\lambda}_3)\alpha'(h)si].\end{aligned} \tag{A41}$$

Define the G function such that

$$\mathcal{G} = u'(c)+(\tilde{\lambda}_2-\tilde{\lambda}_3)\alpha'(h)si. \tag{A42}$$

Solution Strategy

Using the steady state condition $\dot{i}=0, \dot{s}=0$, we have

$$\begin{cases}\alpha(h)s-b-\gamma-\phi+\phi i = 0\\ b-bs-\alpha(h)si+\psi(1-s-i)+\phi si = 0.\end{cases} \tag{A43}$$

we can solve out i and s as functions of h, denoted by $i^*(h), s^*(h)$

Using the F.O.C. $f_1(k, 1-i-\eta(1-s-i)) = r+\delta$, we can solve out k as function of h, denoted by $k^*(h)$.

Using $\dot{k} = 0$ we can solve out $c^*(h)$. Finally, we can express and plot $\mathcal{G}(h)$. We can solve out h^* by $\mathcal{G}(h^*) = 0$.

C HJB

A. General Approach of HJB

- state $X_t \in \mathbb{R}^d$
- control $a_t \in \mathcal{A}$
- value function $V(t, X_t)$
- return function $\mathcal{R}(t, X_t, a_t)$

$$V(t, X_t) = \sup_{a_t} \mathbb{E} \int_t^\infty \mathcal{R}(\tau, X_\tau, a_\tau) d\tau. \tag{A44}$$

By Bellman optimization principle, given a small interval dt

$$\begin{aligned} V(t, X_t) &= \sup_{a_t} \{\mathcal{R}(t, X_t, a_t)dt + \mathbb{E}[V(t + dt, X_{t+dt})]\} \\ 0 &= \sup_{a_t} \{\mathcal{R}(t, X_t, a_t)dt + \mathbb{E}[V(t + dt, X_{t+dt}) - V(t, X_t)]\} \\ 0 &= \sup_{a_t} \{\mathcal{R}(t, X_t, a_t)dt + \mathbb{E}[dV(t, X_t)]\} \\ 0 &= \sup_{a_t} \left\{ \mathcal{R}(t, X_t, a_t)dt + \mathbb{E}\left[\frac{\partial V}{\partial t} dt + \langle \nabla_X V, dX_t \rangle \right] \right\}. \end{aligned} \tag{A45}$$

Cancel out dt, we can specify the HJB as

$$\sup_{a_t} \left\{ \mathcal{R}(t, X_t, a_t) + \mathbb{E}\left[\frac{\partial V}{\partial t} + \langle \nabla_X V, \dot{X}_t \rangle \right] \right\} = 0. \tag{A46}$$

B. Application to the Baseline SIRS/SIR Model

The present value HJB is

$$0 = \sup_{c,h} \left\{ e^{-\rho t} u(c) + \frac{\partial V}{\partial t} + \frac{\partial V}{\partial k}\dot{k} + \frac{\partial V}{\partial i}\dot{i} + \frac{\partial V}{\partial s}\dot{s} \right\}. \tag{A47}$$

We can change the present value HJB to current value

$$0 = \sup_{c,h} \left\{ e^{-\rho t} \left(u(c) + e^{\rho t}\frac{\partial V}{\partial t} + e^{\rho t}\frac{\partial V}{\partial k}\dot{k} + e^{\rho t}\frac{\partial V}{\partial i}\dot{i} + e^{\rho t}\frac{\partial V}{\partial s}\dot{s} \right) \right\}. \tag{A48}$$

Now we define the current value HJB $W = e^{\rho t} V(k, i, s, t)$. We have $\frac{\partial W}{\partial k} = e^{\rho t}\frac{\partial V}{\partial k}$; $\frac{\partial V}{\partial i} = e^{\rho t}\frac{\partial V}{\partial i}$; $\frac{\partial V}{\partial s} = e^{\rho t}\frac{\partial V}{\partial s}$. For $\frac{\partial W}{\partial t}$

$$\begin{aligned}\frac{\partial W}{\partial t} =& e^{\rho t}V + e^{\rho t}\frac{\partial V}{\partial t} \\ =& \rho W + e^{\rho t}\frac{\partial V}{\partial t}.\end{aligned} \tag{A49}$$

Thus, we could rewrite

$$0 = \sup_{c,h}\left\{e^{-\rho t}\left(u(c) + \frac{\partial W}{\partial t} + \frac{\partial W}{\partial k}\dot{k} + \frac{\partial W}{\partial i}\dot{i} + \frac{\partial W}{\partial s}\dot{s} - \rho W\right)\right\}. \tag{A50}$$

The equation

$$0 = \sup_{c,h}\left\{u(c) + \frac{\partial W}{\partial t} + \frac{\partial W}{\partial k}\dot{k} + \frac{\partial W}{\partial i}\dot{i} + \frac{\partial W}{\partial s}\dot{s} - \rho W\right\}, \tag{A51}$$

is the Current Value HJB. PV-HJB and CV-HJB present the same solutions for the control variables as their F.O.C./S.O.C. are identical. Furthermore, We notice that for the CV-HJB

$$W = e^{\rho t}V = \sup_{a_t}\mathbb{E}\int_t^{\infty} e^{-\rho(\tau - t)}u(c_\tau)d\tau. \tag{A52}$$

The time dimension is normalized by t. Thus, the current value W is uncorrelated to time t that $\frac{\partial W}{\partial t} = 0$. Therefore, we could derive the HJB for our baseline model

$$\rho W(k, i, s) = \sup_{c,h}\left\{u(c) + \frac{\partial W}{\partial k}\dot{k} + \frac{\partial W}{\partial i}\dot{i} + \frac{\partial W}{\partial s}\dot{s}\right\}. \tag{A53}$$

The F.O.C. reads

$$\begin{aligned}&u'(c) - \partial_k W = 0 \\ &-\partial_k W + (\partial_i W - \partial_s W)\,\alpha'(h)si = 0.\end{aligned} \tag{A54}$$

We can now see how related between Hamiltonian and HJB. Recall that the $\mathcal{G}(h)$ function in Hamiltonian is

$$\mathcal{G}(h) = u'(c) + (\tilde{\lambda}_s - \tilde{\lambda}_i)\alpha'(h)si, \tag{A55}$$

where $\tilde{\lambda}_s, \tilde{\lambda}_i$ are the co-state for s, i

Manipulate the F.O.C. for HJB we have

$$u'(c) + (\frac{\partial W}{\partial s} - \frac{\partial W}{\partial i})\alpha'(h)si. \tag{A56}$$

C. Application to the Baseline SIRS with Mortality

There would be endogenous discount issue in this case.

Recall that the PV-HJB for value $V = \sup_{c,h} \int_0^\infty e^{-\rho\tau} u(c_\tau) d\tau$ reads

$$0 = \sup_{c,h} \left\{ e^{-\rho t} u(c) + \frac{\partial V}{\partial t} + \frac{\partial V}{\partial k}\dot{k} + \frac{\partial V}{\partial i}\dot{i} + \frac{\partial V}{\partial s}\dot{s} \right\}. \tag{A57}$$

Analogue this expression, for endogenous discount

$$V = \sup_{c,h} \int_t^\infty e^{-\theta_\tau} [u(c_\tau) - \chi(\phi i)] d\tau. \tag{A58}$$

The PV-HJB is

$$0 = \sup_{c,h} \left\{ e^{-\theta} [u(c) - \chi(\phi i)] + \frac{\partial V}{\partial \theta}\dot{\theta} + \frac{\partial V}{\partial k}\dot{k} + \frac{\partial V}{\partial i}\dot{i} + \frac{\partial V}{\partial s}\dot{s} \right\}. \tag{A59}$$

Go through the similar process as the baseline case

$$0 = \sup_{c,h} \left\{ e^{-\theta} \left[[u(c) - \chi(\phi i)] + e^{\theta}\frac{\partial V}{\partial \theta}\dot{\theta} + e^{\theta}\frac{\partial V}{\partial k}\dot{k} + e^{\theta}\frac{\partial V}{\partial i}\dot{i} + e^{\theta}\frac{\partial V}{\partial s}\dot{s} \right] \right\}. \tag{A60}$$

Define $W = e^{\theta} V$, we have

$$\begin{aligned} 0 &= \sup_{c,h} \left\{ e^{-\theta} \left[u(c) - \chi(\phi i) + (\frac{\partial W}{\partial \theta} - W)\dot{\theta} + \frac{\partial W}{\partial k}\dot{k} + \frac{\partial W}{\partial i}\dot{i} + \frac{\partial W}{\partial s}\dot{s} \right] \right\}, \\ 0 &= \sup_{c,h} \left\{ e^{-\theta} \left[u(c) - \chi(\phi i) + \frac{\partial W}{\partial \theta}\dot{\theta} + \frac{\partial W}{\partial k}\dot{k} + \frac{\partial W}{\partial i}\dot{i} + \frac{\partial W}{\partial s}\dot{s} - \dot{\theta} W \right] \right\}. \end{aligned} \tag{A61}$$

Because $\theta = \int_0^t (r - b + d + \phi i_\tau) d\tau$ is not a direct function of the controls c, h, solving

$$0 = \sup_{c,h} \left\{ u(c) - \chi(\phi i) + \frac{\partial W}{\partial \theta}\dot{\theta} + \frac{\partial W}{\partial k}\dot{k} + \frac{\partial W}{\partial i}\dot{i} + \frac{\partial W}{\partial s}\dot{s} - \dot{\theta} W \right\}, \tag{A62}$$

presents the same solution for controls.

D Deep Learning Algorithm

Deep Learning Neural Network (DLNN) approximate the value function. Recall that value function satisfies the HJB

$$u(c^*) + \partial_k V\dot{k} + \partial_i V\dot{i} + \partial_s V\dot{s} - (\rho - b + d)V = 0 \tag{A63}$$

Let $V^{NN}(k, s, i; \Theta)$ as an approximation for $V(k, s, i)$, where Θ is the hyper-parameter for the network. We define the HJB loss

$$Loss_{hjb} = u(c^*) + \partial_k V^{NN}\dot{k} + \partial_i V^{NN}\dot{i} + \partial_s V^{NN}\dot{s} - (\rho - b + d)V^{NN} \tag{A64}$$

Secondly, from FOC (Appendix C Equation A54), and SOC (**??**), we require $\partial_k V > 0$ and $\partial_i V - \partial_s V \leq 0$, we further define the FOC loss and SOC loss as follow

$$\begin{aligned} Loss_{foc} &= \max\{-\partial_k V^{NN}, 0\} \\ Loss_{soc} &= \max\{\partial_i V^{NN} - \partial_s V^{NN}, 0\} \end{aligned} \tag{A65}$$

The Mean Square Loss function is hence

$$MSE(\Theta) = Loss_{hjb}^2 + Loss_{foc}^2 + Loss_{soc}^2 \tag{A66}$$

The deep learning neural network V^{NN} is constructed using the following procedure

- Construct M linear combinition of (k, s, i) i.e. $z_m^{(0)} = \theta_0^{(0)} + \theta_{km}^{(0)}k + \theta_{sm}^{(0)}s + \theta_{im}^{(0)}i; \quad m = 1, 2, 3, ...M$
- Let $\phi^{(1)}(\cdot)$ be any activation function (ReLu, Tanh etc.)
- Construct linear combinition again $z_m^{(1)} = \theta_0^{(1)} + \sum_m \theta_m^{(1)}\phi^{(1)}(z_m^{(0)})$ (First Hidden Layer)
- Construct linear combinition again $z_m^{(2)} = \theta_0^{(2)} + \sum_m \theta_m^{(2)}\phi^{(2)}(z_m^{(1)})$ (Second Hidden Layer)
- etc.
- Deep learning approximation of L layers ($L - 1$ hidden layers) would be

$$v^{NN} = \theta_0^{(L)} + \sum_m \theta_m^{(L)}\phi^{(L)}(z_m^{(L-1)}) \tag{A67}$$

- Figure A11 shows the general structure for neural network

Figure A11. Deep Learning Neural Network

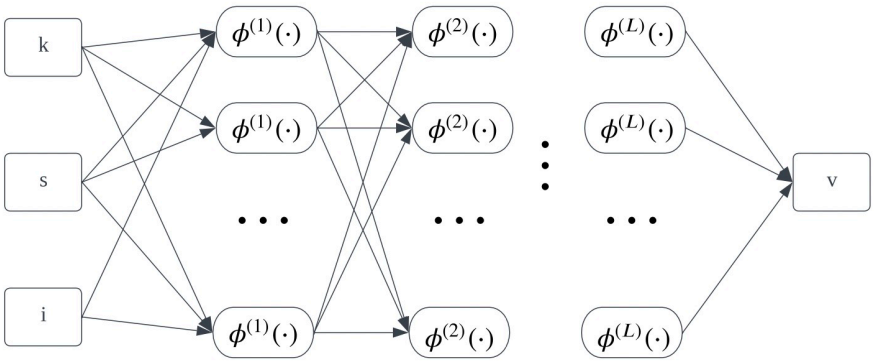

By the **Universal approximation theorem** (Hornik, Stinchcombe, and White, 1989), a neural network with at least one hidden layer can approximate any Borel measurable function mapping finite-dimensional spaces to any desired degree of accuracy. We just need to find proper architecture for the neural network and train the hyper-parameter $\Theta = \{\theta_0^{(0)}...\theta_M^{(J)}\}$ to minimize MSE in Equation A66.

The architecture we select is $M = 10$ neurals, and $L = 7$ hidden layers. We use `ReLu` as the activation function for the first 6 hidden layers and `Tanh` for the last hidden layer. To train the neural network, we apply the Stochastic Gradient Descending (SGD) algorithm with mini-batch of 64[32]. `Adam` (Kingma et al., 2014) with the learning rate of 1e-3 is the optimizer for the training. We also apply 0.001 weight decay to prevent the over-fit problem.

Figure A12 plots the training loss and the verification loss along the convergence path. It shows that both type of losses are sufficiently small. Hence, our neural networks well approximate the HJB equations.

[32]To boost the training efficiency, we draw the mini-batch noramally around the steady state, which is obtained by Hamiltonian in Appendix B

Figure A12. MSE Losses

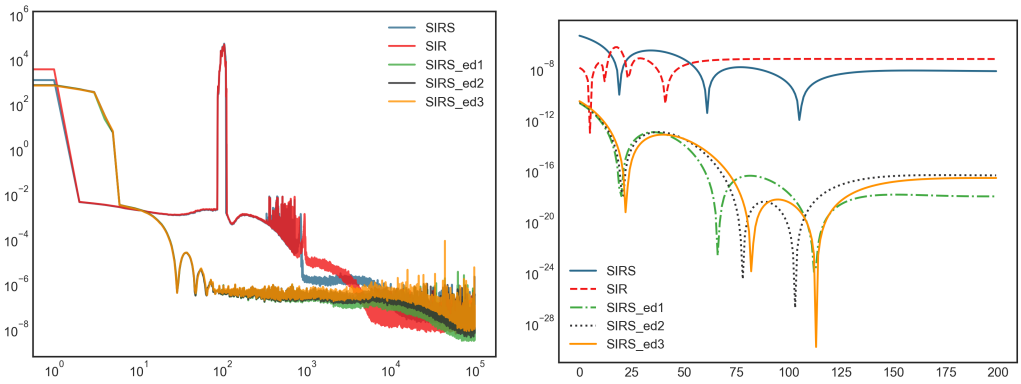

(a) Training Loss **(b)** Verification Loss